

Investigating the Role of Polydopamine to Modulate Stem Cell Adhesion and Proliferation on Gellan Gum-Based Hydrogels

Settimio Pacelli, Patrizia Paolicelli, Stefania Petralito, Siddharth Subham, Drake Gilmore, Gabriele Varani, Guang Yang, Dong Lin, Maria Antonietta Casadei, and Arghya Paul*

Cite This: *ACS Appl. Bio Mater.* 2020, 3, 945–951

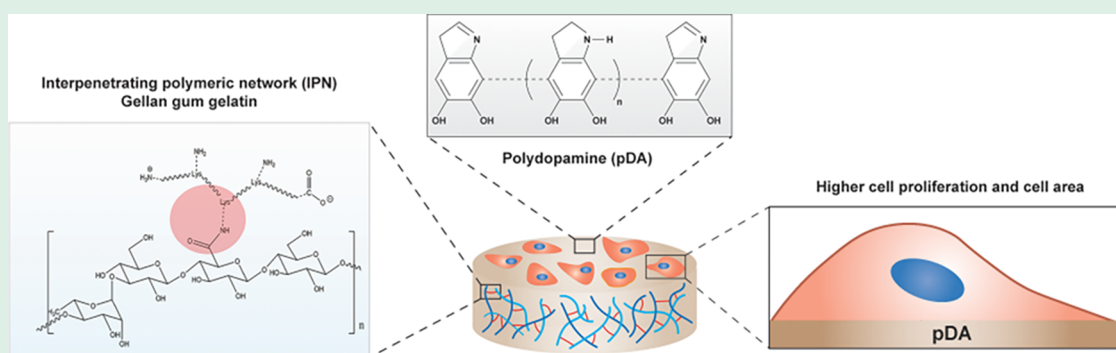
Read Online

ACCESS |

Metrics & More

Article Recommendations

Supporting Information



ABSTRACT: Gellan gum-based hydrogels display limited cell adhesion ability due to the absence of cell-anchorage points usually present in proteins found in the extracellular matrix (ECM). This issue limits their use in the biomedical field as scaffolds to promote tissue repair. Our work addresses this challenge by investigating the use of polydopamine (pDA) as a bioactive layer to improve the surface and biological properties of gellan gum-based hydrogels cross-linked using carbodiimide chemistry. Upon treatment with a pDA layer, the hydrogel displayed an increase in wettability and swelling properties. This change in physical properties had a direct impact on the biological properties of the scaffolds. Precisely, human adipose-derived stem cells (hASCs) seeded on the pDA coated gellan gum hydrogels displayed larger cell area, increased proliferation rate, and enhanced gene expression of focal adhesion and cytoskeletal proteins. Overall, the findings of this research support the use of pDA coating as a possible approach to improve the biological features of gellan gum-based scaffolds and modulate stem cell morphology and proliferation.

KEYWORDS: surface properties, polydopamine coating, stem cell morphology, proliferation, gellan gum hydrogels

1. INTRODUCTION

Polymeric coatings represent an attractive strategy to control the surface of engineered biomaterials.¹ These coatings can display necessary biological factors that can guide cell behavior and the secretion of key signaling molecules.² The direct modulation of stem cell behavior is the basic principle behind the design of cell-instructive materials that will ultimately lead to the discovery of novel therapies for tissue regeneration.³ Bioactive coatings aimed to promote stem cell adhesion can be fabricated using several strategies, including physical adsorption or chemical immobilization of natural proteins found in the extracellular matrix such as fibronectin or collagen.⁴ However, some of these investigated approaches generate coatings with limited stability or require multiple complicated steps that rely on expensive equipment.⁵

A more promising strategy is the use of bioactive molecules that can be polymerized in situ to create adhesive interfaces. One of the most investigated adhesive polymers is polydopamine (pDA), which can be produced by oxidation under alkaline conditions.^{6,7} The coating is fast, reproducible,

uniform, and does not hinder the physical properties of the scaffold. It does not require any toxic condition and is solvent free. Similarly, the process is versatile, and it can be applied ideally to any material such as metal implants, ceramic, and polymeric scaffolds.^{8,9} These advantages make pDA one of the most attractive choices for the design of cell-instructive materials.¹⁰ Furthermore, pDA is biocompatible, and it has been demonstrated to improve cell adhesion and proliferation in various scaffolds, including both natural and synthetic hydrogels.¹¹

Based on these encouraging reports, pDA coatings could be applied to improve the biological properties of existing biomaterials that possess great value in tissue engineering. For example, gellan gum, an anionic extracellular bacterial

Received: October 25, 2019

Accepted: January 1, 2020

Published: January 1, 2020

polysaccharide, has been extensively explored in regenerative medicine to create porous sponges,^{12,13} injectable hydrogels,^{14–16} or bioprinted scaffolds^{17,18} that possess defined porosity, controlled degradability properties, and excellent biocompatibility. However, gellan gum is a bioinert material, with a lack of anchorage points for cell spreading and cellular infiltration, which are essential requirements in many tissue engineering applications such as vascular and bone tissue repair.¹⁹ To overcome this issue, gellan gum-based scaffolds have been modified with ECM proteins or RGD-containing peptides²⁰ to enable direct control over cell morphology and cytoskeletal organization. Unfortunately, these strategies rely on the chemical modification of the scaffold, which is often a multistep, time-consuming process with limited translational potential.

Overall, a simple approach was developed to investigate the role of polydopamine as a modulator of the surface properties of gellan gum hydrogels necessary to influence stem cell morphology and proliferation. We hypothesize that the inclusion of this adhesive coating will have a beneficial impact on the biological features of gellan gum-based scaffolds, which will further extend their applicability in the biomedical field.

2. MATERIALS AND METHODS

2.1. IPN Fabrication and pDA Coating. Hydrogels were fabricated by mixing gellan gum (Gelzan, Mw 1×10^6 , low acetylation degree, Sigma-Aldrich) and gelatin type A (Sigma-Aldrich) in two different ratios 1:5 and 1:10 w/w. Briefly, equal volumes of gelatin (11.1% w/v or 5.5% w/v) and gellan gum (1.1% w/v) solutions in distilled water were mixed at 50 °C before the addition of the chemical cross-linkers. NHS and EDC (Sigma-Aldrich) were used to activate the carboxylic groups of gellan gum and gelatin and enable the formation of amide bonds between the two polymers. Specifically, different degrees of cross-linking were achieved by changing the quantity of the cross-linkers. The reagents were added separately to the polymeric mixture in a 1:1 molar ratio in a range of concentrations varying from 1.55×10^{-2} to 9.30×10^{-2} M. The cross-linkers were mixed for 45 s, and then, the polymers were allowed to fully cross-link for 24 h at 4 °C. Two different interpenetrating polymeric networks were obtained and were identified as IPN (1:5) and IPN (1:10) to indicate the weight ratio between gellan gum and gelatin. The final concentrations of gelatin in the hydrogels were 2.5 and 5% w/v, and the amount of gellan gum was maintained fixed at 0.5% w/v. Physical hydrogels containing both gellan gum and gelatin were obtained without introducing any NHS and EDC into the polymeric mixtures. The IPN hydrogels were immersed in Tris-HCl buffer (pH 8.5) containing dopamine at various concentrations (0.5–2.0 mg/mL). The samples were kept at 37 °C for 1 h and washed thoroughly.

2.2. Rheological, Swelling, and Morphological Characterization. A rotational rheometer (cone and plate geometry) was used to perform the rheological characterization such as frequency sweeps and strain sweeps by following established protocols.^{21,22} Temperature sweeps were performed to verify whether the hydrogels were stable by varying the temperature from 25 to 60 °C (1 °C/min). Experiments were carried out using a constant strain of 0.1% and monitoring the corresponding values of G' and G'' at a frequency of 1 Hz.

Samples were also immersed in phosphate buffer solution ($n = 3$) to study their swelling behavior. Briefly, the hydrogels were swollen in PBS at 37.0 ± 0.1 °C, and the weight was recorded at different time points according to an established procedure.²¹

The porosity of the IPN (1:5) and IPN (1:10) hydrogels with different concentrations of gelatin was observed by scanning electron microscopy (SEM). The samples were prepared based on a protocol reported in another study.²³ Finally, FTIR analysis was carried out on the freeze-dried hydrogels with and without a polydopamine coating following a previous study.²⁴ Briefly, the samples were mixed with KBr

to form a tablet that was directly analyzed (PIKE Technologies, USA). The influence of polydopamine on the hydrophilicity of the surface was monitored by contact angle measurements. Briefly, olive oil drops were placed on the flat surfaces of the coated hydrogels, and the contact angle was quantified using a contact angle analyzer ($n = 5$).

2.3. Release Studies. IPN hydrogels were prepared, and the correct amount of vitamin B12 (5 mg) was solubilized directly in the stock solution of gelatin mixed with gellan gum and the cross-linkers. The hydrogels were placed in PBS (25 mL) at 37.0 ± 0.1 °C. The quantity of vitamin B12 released was determined using HPLC according to an established protocol.²¹ Vitamin B12 was detected at a wavelength of 360 nm using a UV Diode Array Detector (PerkinElmer) ($n = 3$).

A release model was developed to assess the real diffusion coefficient of vitamin B12 from the IPN hydrogel formulations containing different concentrations of gelatin.²⁵ The transport mechanism used to describe the system is composed of a simple diffusion model within the hydrogel (eq 1)

$$\frac{\partial C}{\partial t} = \nabla(D\nabla C) \quad (1)$$

where C is the concentration of vitamin B12 in the reservoir, t is the time, and D is the diffusion coefficient in the hydrogel. A perfect mixing condition was used to describe the reservoir chamber.

2.4. Cell Culture and Proliferation Studies. To investigate the role of polydopamine in influencing the proliferation rate on the hydrogels, the IPN systems were fabricated directly in 24-well plates (1 mL/well) and coated with polydopamine following the procedure reported above. After washing with PBS containing 1% penicillin/streptomycin, 50×10^3 human adipose-derived stem cells (hASCs) (passage 2–6) were seeded and allowed to proliferate for 72 h. Prior to the experiment, hASCs were cultured following an established protocol.²⁶ Hydrogels without any cells were used as control groups to determine the absorbance of the background. Cell proliferation was investigated over 72 h using an MTS assay, and a calibration curve of hASCs from 5×10^3 up to 10×10^4 was obtained to correlate the absorbance obtained from the MTS assay and the number of cells ($n = 5$). Calcein staining was also carried out to visualize the cells on the different hydrogels tested. A fluorescent microscope (Zeiss) was used to collect the fluorescent images at 10 \times magnification.

2.5. Actin-DAPI Staining, Image, and qPCR Analysis. The morphology of hASCs seeded on the hydrogels with and without polydopamine was evaluated after 24 h according to an established protocol.²⁷ The cell area was quantified by tracing the contour of the cells using the software provided with the microscope (ThermoFisher, Scientific USA). At least 10 cells from 5 different images from each group tested ($n = 50$) were analyzed. Additionally, further analysis was carried out using ImageJ software to count the number and length of actin fibers. These parameters were calculated based on at least 10 images per group captured at 20 \times magnification. Only actin stress fibers that were clearly distinguishable from the background were introduced in the calculation.

mRNA was extracted from hASCs seeded on the gels after 24 h postseeding using the instruction provided in the kit (Qiagen). mRNA concentration was quantified, and cDNA was synthesized following an established protocol.²⁸ Primers for RhoA, CDC42, Myo, and paxillin PXN were used along with the miScript SYBR Green Master Mix (Qiagen). The expression of key markers in hASCs seeded on the polydopamine treated group (+pDA) were compared to uncoated hydrogels (–pDA) ($n = 4$).

2.6. Hydroxyapatite Scaffold Printing and Preparation. An established protocol was used to fabricate the hydroxyapatite scaffolds.²⁹ Briefly, a suspension containing 60 w/w of hydroxyapatite was loaded to the syringe which was mounted on a holder so that the printer could control the movement of the syringe. A high precision dispenser was used to apply a stable air pressure, and the extrusion was performed on a hot/cold plate (HCP204SG, Instec, Boulder, CO, USA) with a controlled cooling rate. The samples were transferred to a –70 °C freezer and kept for 12 h. After that, the samples were

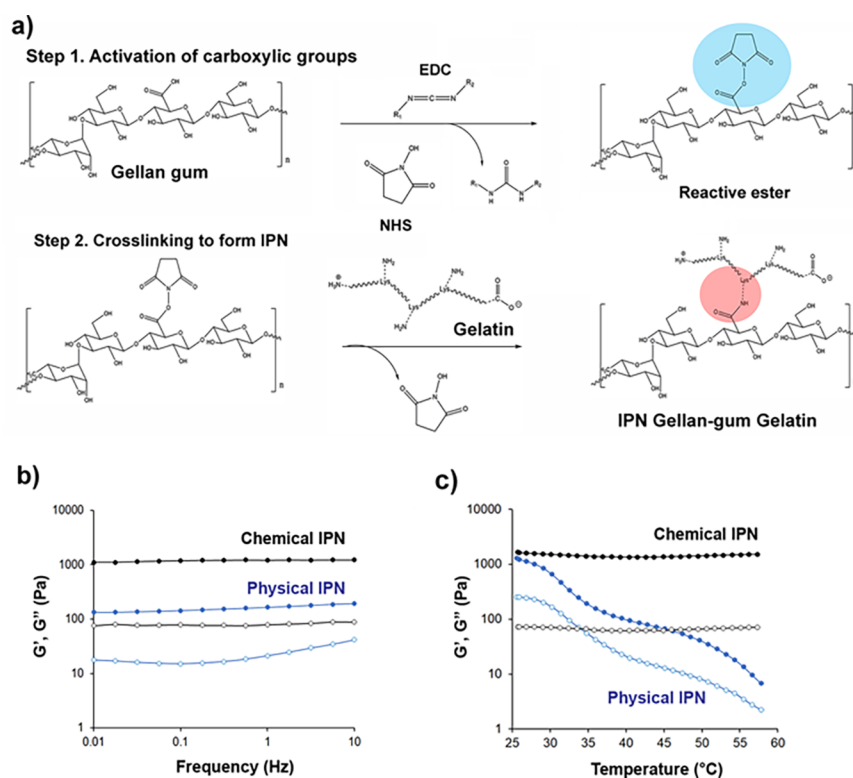


Figure 1. Synthesis and mechanical analysis of the interpenetrated polymeric networks (IPNs). (a) Schematic showing the process of cross-linking between gellan gum and gelatin. (b) Frequency sweep of the chemical and physical IPNs displaying a higher storage modulus (G') in the chemical IPN. (c) Temperature sweep graph showing the thermal stability of the chemical IPN network.

loaded into a freeze-drying system (Labconco, Kansas City, MO) under 200 mPa vacuum at $-35\text{ }^{\circ}\text{C}$ to sublimate ice for 48 h. As the last step, the dried samples were heated at $500\text{ }^{\circ}\text{C}$ for 2 h followed by a treatment at $1300\text{ }^{\circ}\text{C}$ for 3 h.

2.7. Statistical Analysis. A *t*-test or two-way analysis of variance (ANOVA) was carried out according to the number of test groups compared. GraphPad Prism Software 6 was used. Results that were statistically significant were indicated as $*p < 0.05$, $**p < 0.01$, and $***p < 0.001$.

3. RESULTS AND DISCUSSION

3.1. Hydrogel Synthesis and Physical Characterization. The first part of our investigation involved the design of a model platform based on an interpenetrating polymeric network (IPN) of gellan gum and gelatin using the strategy reported in Figure 1a. This chemical strategy was selected because any cytotoxic product can be eliminated by washing the hydrogels.³⁰ Gelatin type A was chosen to enhance the mechanical stability of the hydrogel network and provide RGD amino acid sequences in the hydrogel network necessary to promote the initial step of stem cell adhesion. Additionally, gellan gum alone did not enable the formation of hydrogels using this chemical strategy. The two polymers were chemically cross-linked using NHS/EDC chemistry. Briefly, the cross-linking process consists of the activation of the carboxylic groups of gellan gum into a more reactive intermediate (ester) that will lead to the formation of amide covalent bonds with gelatin. However, it is not possible to exclude the formation of covalent bonds within the gelatin network because of the activation of carboxylic groups in glutamic and aspartic acid. The cross-linking process has been confirmed through rheological studies by monitoring variations in the mechanical properties. NHS/EDC were tested by

keeping the two reagents in the same molar ratio of 1:1, as reported in the Supporting Information (Table S1). The G' values did not significantly change by increasing the concentration of the cross-linkers, as reported in the Supporting Information (Figure S1). An increase of G' from around 100 to 1000 Pa was detected in the optimal hydrogel formulation, as illustrated in Figure 1b. Similarly, we further confirmed the formation of covalent bonds by carrying out temperature sweep tests, as shown in Figure 1c. When the temperature was augmented from 25 to $60\text{ }^{\circ}\text{C}$, the system displayed a decrease in the G' values.

This variation can be attributed to the possible conformational change in the physical entanglement of the two polymers as the temperature increases, leading to a change in the hydrogel stiffness.

On the contrary, this behavior was not observed in the chemically cross-linked system, which presented the same storage module in the entire range of temperatures tested. This finding suggests the obtention of a cross-linked network that possesses the same stiffness irrespective of the temperature used. This feature is extremely important, since changes in stiffness have been reported to directly influence the morphology of stem cells.^{31,32} The obtention of a thermally stable formulation allows the possibility to study stem cell adhesion and cytoskeletal rearrangement excluding the effect of the temperature as a modulator of the stiffness of the designed hydrogel.

The ratio between the two polymers was varied to modulate the stiffness. A ratio of 1:10 was selected based on previous reports discussing the formation of covalent IPN hydrogels obtained by cross-linking gelatin and the polysaccharide alginate in a 1:10 w/w ratio using a similar strategy based on

EDC/NHS chemistry.^{30,33} A ratio of 1:10 w/v resulted in hydrogels with the highest stiffness when compared to the formulation 1:5 (Figure 2a). The higher values of G' could be attributed to the increased level of chain entanglement between the two polymers.

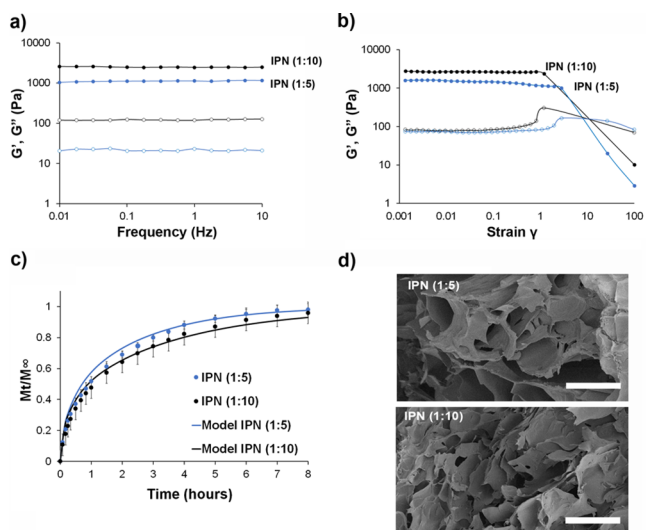


Figure 2. (a) Frequency sweep tests for the two different IPN hydrogels. The IPN systems differ for the amount of gelatin included in the formulation. Specifically, the IPN (1:5) contains gellan gum 0.5% w/v and gelatin 2.5% w/v, while the IPN (1:10) consists of gellan gum 0.5% w/v and gelatin 5% w/v. (b) Strain-sweep profiles displaying the crossover for the different IPN formulations. The IPN (1:10) starts to mechanically fail for lower strain values. (c) Comparison of the experimental and model release data of vitamin B12 from the two different IPN systems ($n = 3$). (d) SEM images of the internal structure of the two IPN systems. Scale bars = 100 μm .

However, the stiffer hydrogel (1:10) was brittle and exhibited a breakage point for lower values of strain, as reported in the strain sweep graphs of Figure 2b. The internal porosity was not influenced by the concentration of gelatin, as confirmed by SEM analysis and by diffusion studies of the model molecule vitamin B12 (Figure 2c,d and Table S2). For all of these reasons, the formulation containing gellan gum 0.5% w/v and gelatin 2.5% w/v (ratio 1:5) was selected for further studies to study the impact of pDA on cell morphology and proliferation.

3.2. Influence of Polydopamine on the Hydrogel Physical Properties. The optimized system was treated with pDA, as illustrated in Figure 3a by following the optimized protocol reported in our previous study using gelatin methacrylamide and alginate.³⁴ The presence of polar groups in both polymers such as hydroxyl, carboxyl, amide, and aromatic side chains masked the presence of the characteristic FTIR bands of pDA. These are commonly found at 3500 cm^{-1} for the stretching of hydroxyl groups and in the region between 1250 and 1600 cm^{-1} , as reported in other studies³⁵ (Figure S2).

The hydrogel surface properties were characterized by contact angle measurements, which is a well-established investigation technique to study the hydrophilicity of the surface of novel materials. Precisely, we observed an increase in the contact angle of olive oil from around 29 to 35° when pDA was varied from 0.5 to 1.0 mg/mL (Figure 3b). Such variation is indicative of a higher level of surface wettability and hydrophilicity. Similar findings have been reported for pDA coated films and fiber-based scaffolds.^{36,37} This effect can be explained by the high hydrophilicity of the pDA coating due to polar catechol/quinone units, amines, and imines.³⁸ This change in hydrophilicity also resulted in a variation in the swelling properties of the hydrogel with a significant increase only in the system coated with 1 mg/mL (Figure 3c). Augmenting the concentration of dopamine to 2 mg/mL did not seem to increase further the swelling properties or the

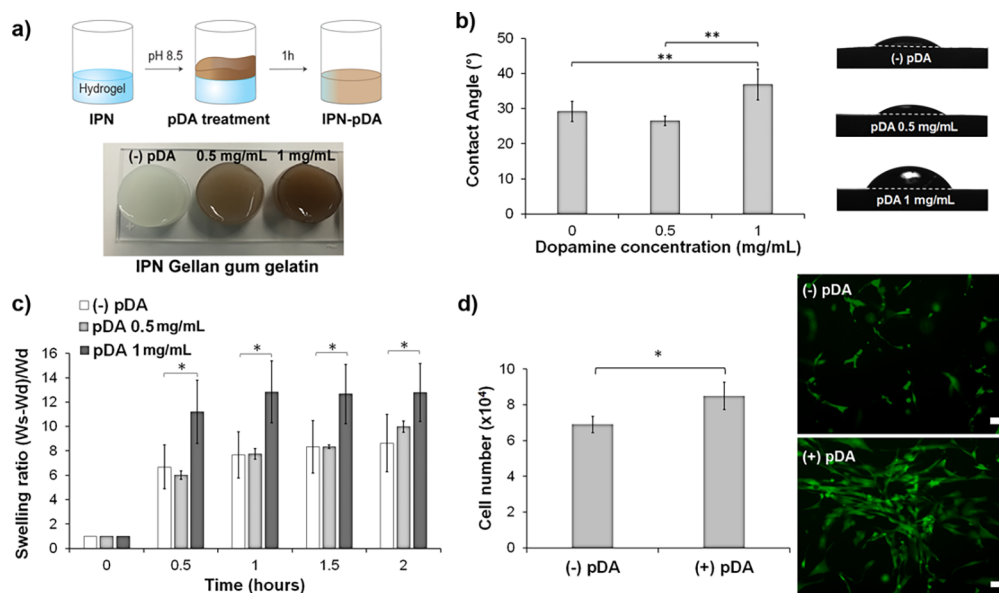


Figure 3. Polydopamine (pDA) treatment to modulate the IPN (1:5) surface properties. (a) Schematic of the process of pDA coating and corresponding images of the coated hydrogels. (b) Contact angle measurements using olive oil and corresponding images of the drop on the surface of the hydrogels ($n = 5$). (c) Swelling results of the hydrogels with the different pDA coatings ($n = 5$). (d) MTS assay results and corresponding calcein staining fluorescent images of hASCs after 72 h. Scale bar = 200 μm . * $p < 0.05$, ** $p < 0.01$.

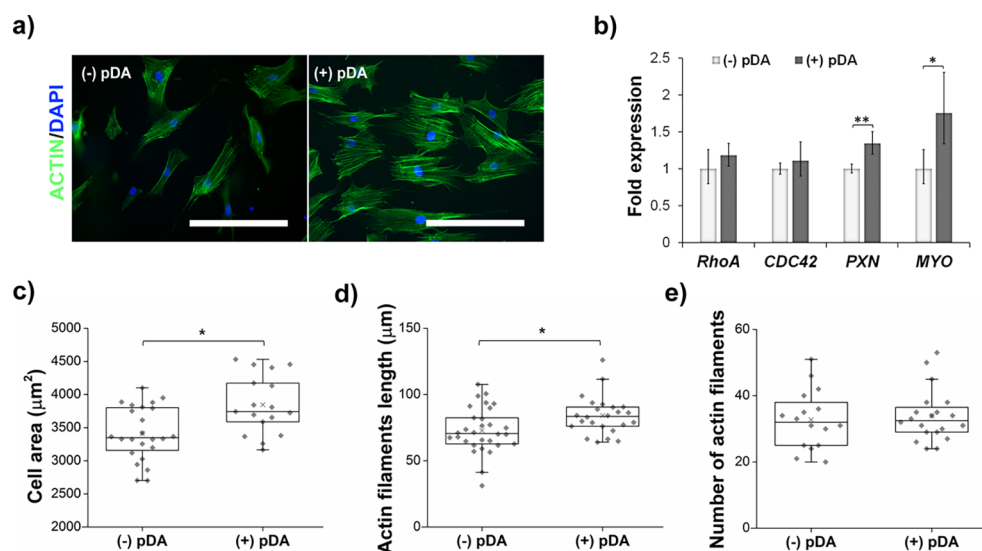


Figure 4. Investigation of the pDA coating on cell morphology. (a) Actin DAPI staining images of hASCs seeded on the IPN (1:5). Scale bar = 200 μm . Images were taken at 20 \times . (b) qPCR analysis of several markers codifying for GTPase proteins RhoA, CDC42, focal adhesion proteins paxillin PXN, and cytoskeletal proteins myosin MYO after 24 h postseeding ($n = 4$). Quantification of (c) cell area, (d) actin filament length, and (e) number of actin filaments in hASCs seeded on the IPN (1:5) with and without a pDA coating. * $p < 0.05$, ** $p < 0.01$.

contact angle of the hydrogel (Figure S3). These results indicate that pDA is indeed capable of altering the hydrophilicity of the hydrogel substrate and this change could be important in modulating serum protein adsorption and indirectly influence stem cell adhesion and cytoskeletal remodeling, as demonstrated in other types of scaffolds.³⁹

3.3. Influence of Polydopamine on Cell Proliferation and Cell Morphology. The optimized coated hydrogels were seeded with hASCs, and this cell line has been selected due to its rapid expansion capability *in vitro*. Cell proliferation was monitored up to 72 h. Interestingly, the inclusion of pDA influenced the proliferation rate of hASCs (Figure 3d) and cell morphology. hASCs started to display a larger shape with visible projections in the (+pDA) compared to the uncoated hydrogels (Figure 4a). Precisely, we observed a larger cell area from an average of 3347 to 3742 μm^2 (Figure 4c). This change in surface area was also combined with a variation in the length of actin fibers, although we did not observe a change in the distribution of their number (Figure 4d,e). Our findings are in accordance with studies examining the effect of pDA on the adhesion and proliferation of human umbilical vein endothelial cells (HUVECs).⁴⁰ It is likely that pDA facilitates the adsorption of serum protein in the medium, which in turn enables the elongation of the cells by facilitating the formation of organized actin-bundles and cell-matrix adhesion points. Moreover, pDA has been reported to enable the adsorption of proteins and retain their native configuration, which is essential for the process of stem cell adhesion and spreading.⁴¹ This indirect effect on the morphology of hASCs was not evident when gelatin was increased from 2.5 to 5% w/v IPN (1:10), indicating how the inclusion of a larger number of anchorage adhesion points provided by the RGD sequences of gelatin is the primary factor influencing hASC morphology in the IPN (1:10) formulation (Figure S4). However, an increase in cell proliferation was found in the IPN (1:10) coated with a pDA layer (Figure S5).

To further prove the modulatory impact of the pDA coating on hASC, we also performed a qPCR analysis of the main markers regulating adhesion, actin–myosin remodeling, and

cell–matrix interactions (Figure 4b). Interestingly, RhoA and CDC42 expression were similar among the two groups tested after 24 h postseeding. These genes codify for small GTPase proteins that regulate cytoskeletal remodeling, actin contractility, and cell cycle division. Upregulation of these genes is commonly observed in response to a change in substrate stiffness,⁴² and it is likely that the inclusion of the pDA coating did not affect the stiffness of the IPN system significantly. On the contrary, another study reported an enhancement in this parameter for gellan gum-based hydrogels after treatment with pDA, which also contributed to enhanced mineralization upon incorporation of alkaline phosphatase within the hydrogels.⁴³ However, it should be noted that the mechanism of cross-linking reported in this study was not based on the use of calcium ions, which can be complexed by the catechol units present within the pDA structure.

The presence of the pDA coating enhanced the expression of paxillin, which is one of the key proteins found in the focal adhesion complex, which provides the anchorage between cells and the substrate.^{44,45} This increase in paxillin expression has also been found in other reports displaying how pDA can influence the formation of a larger amount of focal adhesions. Similarly, the overexpression of the marker MYO, which codifies for the expression of myosin in the cytoskeleton, suggests how the presence of pDA can facilitate the reorganization of actin–myosin filaments which are essential for the formation of cell–matrix interactions.⁴⁵

4. CONCLUSIONS

Overall, the pDA coating positively modulated the surface properties of the IPN hydrogels and induced a higher proliferation and cell spreading. These findings support the possible use of pDA as a valid strategy to extend the potential of gellan gum-based hydrogels for tissue engineering applications. Finally, the optimized hydrogel formulation IPN (1:5) can also be used as an intermediate layer coating to modulate the surface and biological properties of prefabricated scaffolds made of hydroxyapatite (Figure S6). Further studies will be carried out to investigate whether the optimized

hydrogel coating in combination with a pDA layer can be used to enhance the osteogenic differentiation of hydroxyapatite scaffolds to generate a cell-instructive interface for bone tissue regeneration.

■ ASSOCIATED CONTENT

Supporting Information

The Supporting Information is available free of charge at <https://pubs.acs.org/doi/10.1021/acsabm.9b00989>.

A table summarizing the different temperatures of gelation based on different concentrations of EDC/NHS, frequency sweeps of gellan gum-based hydrogels with different NHS/EDC concentrations, a table showing the diffusion coefficient of vitamin B12 from 1:5 and 1:10 IPN hydrogels, FTIR of hydrogel with and without pDA coating, swelling and contact angle measurements for 1:10 IPN hydrogels, cell study on 1:10 IPN hydrogels, and preliminary results showing the coating of prefabricated scaffolds of hydroxyapatite with the optimized IPN hydrogels (PDF)

■ AUTHOR INFORMATION

Corresponding Author

Arghya Paul – The University of Western Ontario, London, Canada; orcid.org/0000-0003-4788-0378; Email: arghya.paul@uwo.ca

Other Authors

Settimio Pacelli – University of Kansas, Lawrence, Kansas; orcid.org/0000-0002-4879-3615

Patrizia Paolicelli – Sapienza University of Rome, Rome, Italy

Stefania Petralito – Sapienza University of Rome, Rome, Italy

Siddharth Subham – University of Kansas, Lawrence, Kansas

Drake Gilmore – University of Kansas, Lawrence, Kansas

Gabriele Varani – IEIIT Institute, Genoa, Italy

Guang Yang – Kansas State University, Manhattan, Kansas

Dong Lin – Kansas State University, Manhattan, Kansas

Maria Antonietta Casadei – Sapienza University of Rome, Rome, Italy

Complete contact information is available at: <https://pubs.acs.org/doi/10.1021/acsabm.9b00989>

Notes

The authors declare no competing financial interest.

■ ACKNOWLEDGMENTS

The authors would like to acknowledge the University of Kansas for granting the funding necessary for the realization of this work. A.P. acknowledges the financial support received from the Canada Research Chairs Program of the Natural Sciences and Engineering Research Council (NSERC) of Canada. D.L. would like to acknowledge the financial support obtained from the National Science Foundation under the Award No. OIA-1656006. Similarly, D.L. would like to acknowledge the support from the State of Kansas through

the Kansas Board of Regents. The authors would like to thank Prof. Stevin Gehrke for granting access to his instruments.

■ REFERENCES

- (1) Chen, L.; Yan, C.; Zheng, Z. Functional polymer surfaces for controlling cell behaviors. *Mater. Today* **2018**, *21* (1), 38–59.
- (2) Custódio, C. A.; Reis, R. L.; Mano, J. F. Engineering Biomolecular Microenvironments for Cell Instructive Biomaterials. *Adv. Healthcare Mater.* **2014**, *3* (6), 797–810.
- (3) Murphy, W. L.; McDevitt, T. C.; Engler, A. J. Materials as stem cell regulators. *Nat. Mater.* **2014**, *13*, 547.
- (4) Pacelli, S.; Manoharan, V.; Desalvo, A.; Lomis, N.; Jodha, K. S.; Prakash, S.; Paul, A. Tailoring biomaterial surface properties to modulate host-implant interactions: implication in cardiovascular and bone therapy. *J. Mater. Chem. B* **2016**, *4* (9), 1586–1599.
- (5) Bishop, C. A. Polymer Coating Basic Information. In *Vacuum Deposition onto Webs, Films and Foils* (2nd ed.); Bishop, C. A., Ed.; William Andrew Publishing: Oxford, U.K., 2011; pp 197–214.
- (6) Kord Forooshani, P.; Lee, B. P. Recent approaches in designing bioadhesive materials inspired by mussel adhesive protein. *J. Polym. Sci., Part A: Polym. Chem.* **2017**, *55* (1), 9–33.
- (7) Hong, S.; Na, Y. S.; Choi, S.; Song, I. T.; Kim, W. Y.; Lee, H. Non-Covalent Self-Assembly and Covalent Polymerization Co-Contribute to Polydopamine Formation. *Adv. Funct. Mater.* **2012**, *22* (22), 4711–4717.
- (8) Liu, Y.; Ai, K.; Lu, L. Polydopamine and Its Derivative Materials: Synthesis and Promising Applications in Energy, Environmental, and Biomedical Fields. *Chem. Rev.* **2014**, *114* (9), 5057–5115.
- (9) Ryu, J. H.; Messersmith, P. B.; Lee, H. Polydopamine Surface Chemistry: A Decade of Discovery. *ACS Appl. Mater. Interfaces* **2018**, *10* (9), 7523–7540.
- (10) Wang, R.; Li, J.; Chen, W.; Xu, T.; Yun, S.; Xu, Z.; Sato, T.; Chi, B.; Xu, H. A Biomimetic Mussel-Inspired ϵ -Poly-L-lysine Hydrogel with Robust Tissue-Anchor and Anti-Infection Capacity. *Adv. Funct. Mater.* **2017**, *27* (8), 1604894.
- (11) Ding, Y. H.; Floren, M.; Tan, W. Mussel-inspired polydopamine for bio-surface functionalization. *Biosurface and Biotribology* **2016**, *2* (4), 121–136.
- (12) Chang, S. J.; Huang, Y.-T.; Yang, S.-C.; Kuo, S.-M.; Lee, M.-W. In vitro properties of gellan gum sponge as the dental filling to maintain alveolar space. *Carbohydr. Polym.* **2012**, *88* (2), 684–689.
- (13) da Silva, L. P.; Cerqueira, M. T.; Sousa, R. A.; Reis, R. L.; Corrello, V. M.; Marques, A. P. Engineering cell-adhesive gellan gum spongy-like hydrogels for regenerative medicine purposes. *Acta Biomater.* **2014**, *10* (11), 4787–4797.
- (14) Pacelli, S.; Paolicelli, P.; Dreesen, I.; Kobayashi, S.; Vitalone, A.; Casadei, M. A. Injectable and photocross-linkable gels based on gellan gum methacrylate: A new tool for biomedical application. *Int. J. Biol. Macromol.* **2015**, *72*, 1335–1342.
- (15) Oliveira, J. T.; Gardel, L. S.; Rada, T.; Martins, L.; Gomes, M. E.; Reis, R. L. Injectable gellan gum hydrogels with autologous cells for the treatment of rabbit articular cartilage defects. *J. Orthop. Res.* **2010**, *28* (9), 1193–1199.
- (16) Du, H.; Hamilton, P.; Reilly, M.; Ravi, N. Injectable in situ physically and chemically crosslinkable gellan hydrogel. *Macromol. Biosci.* **2012**, *12* (7), 952–61.
- (17) Wu, D.; Yu, Y.; Tan, J.; Huang, L.; Luo, B.; Lu, L.; Zhou, C. 3D bioprinting of gellan gum and poly (ethylene glycol) diacrylate based hydrogels to produce human-scale constructs with high-fidelity. *Mater. Des.* **2018**, *160*, 486–495.
- (18) Hu, D.; Wu, D.; Huang, L.; Jiao, Y.; Li, L.; Lu, L.; Zhou, C. 3D bioprinting of cell-laden scaffolds for intervertebral disc regeneration. *Mater. Lett.* **2018**, *223*, 219–222.
- (19) Ferris, C. J.; Gilmore, K. J.; Wallace, G. G.; Panhuis, M. i. h. Modified gellan gum hydrogels for tissue engineering applications. *Soft Matter* **2013**, *9* (14), 3705–3711.
- (20) Silva, N. A.; Cooke, M. J.; Tam, R. Y.; Sousa, N.; Salgado, A. J.; Reis, R. L.; Shoichet, M. S. The effects of peptide modified gellan gum

and olfactory ensheathing glia cells on neural stem/progenitor cell fate. *Biomaterials* **2012**, *33* (27), 6345–6354.

(21) Pacelli, S.; Paolicelli, P.; Pepi, F.; Garzoli, S.; Polini, A.; Tita, B.; Vitalone, A.; Casadei, M. A. Gellan gum and polyethylene glycol dimethacrylate double network hydrogels with improved mechanical properties. *J. Polym. Res.* **2014**, *21* (5), 409.

(22) Pacelli, S.; Paolicelli, P.; Avitabile, M.; Varani, G.; Di Muzio, L.; Cesa, S.; Tirillò, J.; Bartuli, C.; Nardoni, M.; Petralito, S.; Adrover, A.; Casadei, M. A. Design of a tunable nanocomposite double network hydrogel based on gellan gum for drug delivery applications. *Eur. Polym. J.* **2018**, *104*, 184–193.

(23) Pacelli, S.; Acosta, F.; Chakravarti, A. R.; Samanta, S. G.; Whitlow, J.; Modaresi, S.; Ahmed, R. P. H.; Rajasingh, J.; Paul, A. Nanodiamond-based injectable hydrogel for sustained growth factor release: Preparation, characterization and in vitro analysis. *Acta Biomater.* **2017**, *58*, 479–491.

(24) Pacelli, S.; Maloney, R.; Chakravarti, A. R.; Whitlow, J.; Basu, S.; Modaresi, S.; Gehrke, S.; Paul, A. Controlling Adult Stem Cell Behavior Using Nanodiamond-Reinforced Hydrogel: Implication in Bone Regeneration Therapy. *Sci. Rep.* **2017**, *7* (1), 6577.

(25) Chowdhury, M. A.; Hill, D. J. T.; Whittaker, A. K. Vitamin B12 Release from P(HEMA-co-THFMA) in Water and SBF: A Model Drug Release Study. *Aust. J. Chem.* **2005**, *58* (6), 451–456.

(26) Modaresi, S.; Pacelli, S.; Subham, S.; Dathathreya, K.; Paul, A. Intracellular Delivery of Exogenous Macromolecules into Human Mesenchymal Stem Cells by Double Deformation of the Plasma Membrane. *Advanced Therapeutics* **2019**, 1900130.

(27) Basu, S.; Pacelli, S.; Feng, Y.; Lu, Q.; Wang, J.; Paul, A. Harnessing the Noncovalent Interactions of DNA Backbone with 2D Silicate Nanodisks To Fabricate Injectable Therapeutic Hydrogels. *ACS Nano* **2018**, *12* (10), 9866–9880.

(28) Waters, R.; Subham, S.; Pacelli, S.; Modaresi, S.; Chakravarti, A. R.; Paul, A. Development of MicroRNA-146a-Enriched Stem Cell Secretome for Wound-Healing Applications. *Mol. Pharmaceutics* **2019**, *16* (10), 4302–4312.

(29) Song, X.; Tetik, H.; Jirakittsonthon, T.; Parandoush, P.; Yang, G.; Lee, D.; Ryu, S.; Lei, S.; Weiss, M. L.; Lin, D. Biomimetic 3D Printing of Hierarchical and Interconnected Porous Hydroxyapatite Structures with High Mechanical Strength for Bone Cell Culture. *Adv. Eng. Mater.* **2019**, *21* (1), 1800678.

(30) Pacelli, S.; Basu, S.; Berkland, C.; Wang, J.; Paul, A. Design of a Cytocompatible Hydrogel Coating to Modulate Properties of Ceramic-Based Scaffolds for Bone Repair. *Cell. Mol. Bioeng.* **2018**, *11* (3), 211–217.

(31) Charrier, E. E.; Pogoda, K.; Wells, R. G.; Janmey, P. A. Control of cell morphology and differentiation by substrates with independently tunable elasticity and viscous dissipation. *Nat. Commun.* **2018**, *9* (1), 449.

(32) Modaresi, S.; Pacelli, S.; Whitlow, J.; Paul, A. Deciphering the role of substrate stiffness in enhancing the internalization efficiency of plasmid DNA in stem cells using lipid-based nanocarriers. *Nanoscale* **2018**, *10* (19), 8947–8952.

(33) Yang, C.; Frei, H.; Rossi, F. M.; Burt, H. M. The differential in vitro and in vivo responses of bone marrow stromal cells on novel porous gelatin-alginate scaffolds. *J. Tissue Eng. Regen. Med.* **2009**, *3* (8), 601–614.

(34) Pacelli, S.; Rampetsreiter, K.; Modaresi, S.; Subham, S.; Chakravarti, A. R.; Lohfeld, S.; Detamore, M. S.; Paul, A. Fabrication of a Double-Cross-Linked Interpenetrating Polymeric Network (IPN) Hydrogel Surface Modified with Polydopamine to Modulate the Osteogenic Differentiation of Adipose-Derived Stem Cells. *ACS Appl. Mater. Interfaces* **2018**, *10* (30), 24955–24962.

(35) Liebscher, J.; Mrówczyński, R.; Scheidt, H. A.; Filip, C.; Hädade, N. D.; Turcu, R.; Bende, A.; Beck, S. Structure of Polydopamine: A Never-Ending Story? *Langmuir* **2013**, *29* (33), 10539–10548.

(36) Shin, Y. M.; Lee, Y. B.; Shin, H. Time-dependent mussel-inspired functionalization of poly(L-lactide-co-ε-caprolactone)

substrates for tunable cell behaviors. *Colloids Surf., B* **2011**, *87* (1), 79–87.

(37) Ku, S. H.; Park, C. B. Human endothelial cell growth on mussel-inspired nanofiber scaffold for vascular tissue engineering. *Biomaterials* **2010**, *31* (36), 9431–7.

(38) Jia, L.; Han, F.; Wang, H.; Zhu, C.; Guo, Q.; Li, J.; Zhao, Z.; Zhang, Q.; Zhu, X.; Li, B. Polydopamine-assisted surface modification for orthopaedic implants. *Journal of Orthopaedic Translation* **2019**, *17*, 82–95.

(39) Yang, K.; Lee, J. S.; Kim, J.; Lee, Y. B.; Shin, H.; Um, S. H.; Kim, J. B.; Park, K. I.; Lee, H.; Cho, S. W. Polydopamine-mediated surface modification of scaffold materials for human neural stem cell engineering. *Biomaterials* **2012**, *33* (29), 6952–64.

(40) Wang, J. L.; Ren, K. F.; Chang, H.; Jia, F.; Li, B. C.; Ji, Y.; Ji, J. Direct adhesion of endothelial cells to bioinspired poly(dopamine) coating through endogenous fibronectin and integrin α5β1. *Macromol. Biosci.* **2013**, *13* (4), 483–93.

(41) Ku, S. H.; Ryu, J.; Hong, S. K.; Lee, H.; Park, C. B. General functionalization route for cell adhesion on non-wetting surfaces. *Biomaterials* **2010**, *31* (9), 2535–41.

(42) Lv, H.; Li, L.; Sun, M.; Zhang, Y.; Chen, L.; Rong, Y.; Li, Y. Mechanism of regulation of stem cell differentiation by matrix stiffness. *Stem Cell Res. Ther.* **2015**, *6* (1), 103.

(43) Douglas, T. E.; Włodarczyk, M.; Pamula, E.; Declercq, H. A.; de Mulder, E. L.; Bucko, M. M.; Balcaen, L.; Vanhaecke, F.; Cornelissen, R.; Dubruel, P.; Jansen, J. A.; Leeuwenburgh, S. C. Enzymatic mineralization of gellan gum hydrogel for bone tissue-engineering applications and its enhancement by polydopamine. *J. Tissue Eng. Regen. Med.* **2014**, *8* (11), 906–18.

(44) Fraley, S. I.; Feng, Y.; Krishnamurthy, R.; Kim, D.-H.; Celedon, A.; Longmore, G. D.; Wirtz, D. A distinctive role for focal adhesion proteins in three-dimensional cell motility. *Nat. Cell Biol.* **2010**, *12*, 598.

(45) Geiger, B.; Spatz, J. P.; Bershadsky, A. D. Environmental sensing through focal adhesions. *Nat. Rev. Mol. Cell Biol.* **2009**, *10* (1), 21–33.